Track-before-detect algorithm for maneuvering infrared weak multiple targets via particle filter

Yinsheng Zhang (张寅生), Yunli Long (龙云利)*, and Kun Liu (刘 琨)

College of Aerospace Science and Engineering, National University of Defense Technology, Changsha 410007, China

**Corresponding author: feiyunlyi@126.com*

Received April 27, 2014; accepted June 18, 2014; posted online September 28, 2014

We present a particle filter (PF)-based algorithm to detect and track maneuvering infrared weak multiple targets at different signal-to-noise ratios for the scenes with the multiple targets number unknown and varying. A detecting filter and a tracking filter based on sequential likelihood ratio (LR) testing with fixed sample size are designed, respectively, for capturing new target and tracking confirmed targets. The algorithm is optimized with selectively particles sampling and adaptive process noise. Targets birth and death time are accurately estimated according to the change degree of the LR along with the corresponding state amended through PF backward recursion. Simulation results show that it is positive to detect and track maneuvering infrared weak multiple targets with the appearance and disappearance of more than one, which also achieves a significant improvement in state estimation especially for the time targets which appear and disappear.

OCIS codes: 110.3080, 100.2960, 100.4999, 200.3050.

doi: 10.3788/COL201412.101101.

Detecting and tracking maneuvering dim targets is the focus of infrared sensors data processing. Track-before-detect (TBD) algorithms use the entire output without information loss, avoiding the typical measurement pre-threshold and data association, which gain better detection performance than the classical detect-before-track methods.

Boers *et al.*[1] proposed particle filter (PF) for TBD, which has been proved by Davey *et al.*[2] to outperform histogram probability multi-hypothesis tracking (H-PMHT)[3,4] and probabilistic data association (PDA)[5] regardless of computation cost. And it is extended for two targets based on sequential likelihood ratio testing (SLRT) of three hypotheses[1,6]. However, the number of targets present is unknown and even time variant. Then it should be modified by composite multi-hypothesis testing or heuristic searching, which is complex and time-consuming. Pertilä[7] presented an improved algorithm based on PF for multiple targets. However it is assumed that there is not more than one target appearing or disappearing simultaneously. So the improved algorithm is not suitable when more than one target appear or disappear. Morelande *et al.*[8] detected and tracked targets by the computation of the joint multi-target probability density. The algorithm seems to detect and track unknown number of targets. Buzzi *et al.*[9] proposed a Viterbi-like algorithm based on generalized likelihood ratio test (GLRT) and extended it for multiple targets with known target number N_k at time step k via dynamic programming and an equivalent minimum network flow optimization. It should be solved by composite multi-hypothesis testing[9] for multiple targets with N_k unknown. And it is extended in the context of space-time adaptive processing[10] without the incorporation of the target kinematics. A one-step GLRT-based detector for varying scenario and ad hoc detectors for both stationary and varying scenarios are derived and further extended for bistatic sonars[11,12]. Although they could be extended for multiple targets with N_k unknown by introducing composite multi-hypothesis testing, it would become very complex and not work well when N_k are number varying and maneuvering.

Probability hypothesis density (PHD) is proposed based on random finite set for tracking multiple targets[13], which can efficiently estimate the target number and state simultaneously. A sequential Monte Carlo-PHD (SMC-PHD) is designed by Vo *et al.*[14] and multiple model PHD (MM-PHD)[15] is presented consequently for maneuvering targets. A SMC-PHD TBD-based algorithm is proposed to track low-observable multiple targets[16]. Improved MM-PHD algorithms are proposed for detecting and tracking multiple targets with N_k unknown by Long *et al.*[17,18]. The algorithms are effective for maneuvering targets with varying N_k. However, the implementation of the algorithms is complicated with large computation and both the birth and death time of targets are not accurately captured. Usually the data association should be implemented for tracking a continuous trace with low false alarm rate.

In order to detect and track multiple weak targets with N_k unknown and varying, we present an effective algorithm based on PF, which incorporates a filter for detecting new target and a second filter for tracking conformed targets. And optimization is conducted on the estimation of the target birth and death time and corresponding state in parallel with not only selectively sampling but also adaptive process noise.

Given the model of the target falls into the cluster of constant velocity (CV), clockwise constant turn

(C-CT), and anticlockwise constant turn (AC-CT), the evolution of the target state is modeled as a linear Gaussian dynamic system:

$$\mathrm{X}_k = F^{(i)}\left(\mathrm{X}_{k-1}\right)\mathrm{X}_{k-1} + \mathrm{v}_k^i, \tag{1}$$

where the target state at time k is composed of five components referring to position and position rate in two directions along with the amplitude, which can be written as

$$\mathrm{X}_k = \left[x_k, \dot{x}_k, y_k, \dot{y}_k, I_k\right]^T. \tag{2}$$

As depicted in Ref. [19], $F^{(i)}$ denotes the state dynamic function with superscript i representing the mode index, whose transition is modeled by a Markov chain with matrix $\mathbf{\Pi}$. Process noise v_k^i is Gaussian distributed with zero mean and covariance Q_k^i.

For each cell of the infrared sensor, indexed by $i \in \left[1, W\right]$ and $j \in \left[1, H\right]$, its amplitude under N targets in existence is modeled by

$$\mathrm{Z}_k^{(i,j)} = \sum\nolimits_{n=1}^{N} h_k^{(i,j)}\left(\mathrm{X}_k^{(n)}, \mathrm{u}_k\right) + \mathrm{n}_k^{(i,j)}, \tag{3}$$

where the noise $\mathbf{n}_k^{(i,j)}$ independent between cells is Gaussian with variance σ^2 and $\mathrm{u}_k = \left[\Delta_k^x, \Delta_k^y\right]$ stands for imaging position errors on the focal plane array due to inaccuracy of the line of sight and the like. The contribution to the cell (i, j) from the target n at time k is functioned as

$$h_k^{(i,j)}\left(\mathbf{X}_k^{(n)}, \mathbf{u}_k\right) = \int_{i-1}^{i}\int_{j-1}^{j} \frac{I_k^{(n)}}{2\pi\Sigma^2} \times \exp\left(\frac{-\left(x - x_k^{(n)} - \Delta_k^x\right)^2 - \left(y - y_k^{(n)} - \Delta_k^y\right)^2}{2\Sigma^2}\right)\mathrm{d}x\,\mathrm{d}y, \tag{4}$$

where Σ denotes the parameter for the point spread function. The peak signal-to-noise ratio (SNR) for the target written as $\mathrm{SNR_T}$ is given by[2]

$$\mathrm{SNR_T} = 20\log\left(I_k^{(n)}\right) - 20\log\left(2\pi\sigma\Sigma^2\right). \tag{5}$$

However, the peak SNR for the pixel written as $\mathrm{SNR_P}$ is given by

$$\mathrm{SNR_P} = 20\log\left(I_{\max,k}^{(n)}\right) - 20\log\left(2\pi\sigma\Sigma^2\right), \tag{6}$$

where $I_{\max,k}^{(n)}$ is the maximum energy in one cell when the target lies in the center of it and is given as

$$I_{\max,k}^{(n)} = \int_{x_k^{(n)}-0.5}^{x_k^{(n)}+0.5}\int_{y_k^{(n)}-0.5}^{y_k^{(n)}+0.5} \frac{I_k^{(n)}}{2\pi\Sigma^2} \times \exp\left(\frac{-\left(x - x_k^{(n)}\right)^2 - \left(y - y_k^{(n)}\right)^2}{2\Sigma^2}\right)\mathrm{d}x\,\mathrm{d}y. \tag{7}$$

PF-TBD for single target is settled through binary hypothesis testing based on SLRT:

H0: no target

$$\mathrm{Z}_k^{(i,j)} = \mathrm{n}_k^{(i,j)}.$$

H1: target present:

$$\mathrm{Z}_k^{(i,j)} = h_k^{(i,j)}\left(\mathrm{X}_k, \mathrm{u}_k\right) + \mathrm{n}_k^{(i,j)}.$$

The complete measurements at time k are given by $\mathrm{Z}_k = \left\{\mathrm{Z}_k^{(i,j)} \middle| i = 1\cdots W, j = 1\cdots H\right\}$, the likelihood ratio (LR) of which can be written as

$$L\left(\mathbf{Z}_k\left(\mathbf{X}_k\right)\right) = \frac{P\left(\mathbf{Z}_k \middle| H_1\right)}{P\left(\mathbf{Z}_k \middle| H_0\right)}. \tag{8}$$

Given the spread of the target limited to several cells near the central target bin, LR is approximated by

$$L\left(\mathrm{Z}_k\left(\mathrm{X}_k\right)\right) \approx \prod_{i\in C_i\left(\mathrm{X}_k\right)}\prod_{i\in C_j\left(\mathrm{X}_k\right)} \frac{P\left(\mathrm{Z}_k^{(i,j)} \middle| H_1\right)}{P\left(\mathrm{Z}_k^{(i,j)} \middle| H_0\right)}, \tag{9}$$

where $C_i\left(\mathbf{X}_k\right)$ and $C_j\left(\mathbf{X}_k\right)$ are the set of the cell indices spread by the target in the x and y dimensions, respectively. According to Ref. [1], LR is characterized by the un-normalized weight of the particles:

$$L\left(\mathrm{Z}_k\left(\mathrm{X}_k\right)\right) \approx \frac{1}{N_p}\sum\nolimits_{l=1}^{N_p} \tilde{q}_k^l, \tag{10}$$

where N_p is the number of the particles.

Denote the measurements up to time k as $\mathrm{Z}^k = \left\{\mathrm{Z}_1, \mathrm{Z}_2 \cdots \mathrm{Z}_k\right\}$. For the independency of the measurements at different time, the cumulative LR is

$$\Lambda\left(\mathrm{Z}^k\left(\mathrm{X}_{1\cdots k}\right)\right) = \prod_{i=1\cdots k} L\left(\mathrm{Z}_i\left(\mathrm{X}_i\right)\right), \tag{11}$$

where usually SLRT is adopted with fixed sample size (FSS) M as:

$$\Lambda^{\mathrm{FSS}}\left(\mathrm{Z}^k\left(\mathrm{X}_{k-M\cdots k}\right)\right) = \prod_{i=k-M\cdots k} L\left(\mathrm{Z}_i\left(\mathrm{X}_i\right)\right). \tag{12}$$

Therefore

$$\Lambda^{\mathrm{FSS}}\left(\mathbf{Z}^k\left(\mathbf{X}_{k-M\cdots k}\right)\right) \approx \Lambda^{\mathrm{FSS}}\left(\mathbf{Z}^{k-1}\left(\mathbf{X}_{k-M\cdots k-1}\right)\right) \frac{1}{N_p}\sum\nolimits_{l=1}^{N_p} \tilde{q}_k^l. \tag{13}$$

The logarithmic form of the above formula is

$$\log\left(\Lambda^{\mathrm{FSS}}\left(\mathrm{Z}^k\left(\mathrm{X}_{k-M\cdots k}\right)\right)\right) \approx \log\left(\Lambda^{\mathrm{FSS}}\left(\mathrm{Z}^{k-1}\left(\mathrm{X}_{k-M\cdots k-1}\right)\right)\right) + \log\left(\frac{1}{N_p}\sum\nolimits_{l=1}^{N_p} \tilde{q}_k^l\right). \tag{14}$$

The target detection becomes

$$\log\left(\Lambda^{\mathrm{FSS}}\left(\mathrm{Z}^k\right)\right)\begin{cases} \geq \log\left(\eta_1\right) & \text{, accept } H_1 \\ \leq \log\left(\eta_0\right) & \text{, accept } H_0 \\ \in \left(\log\left(\eta_0\right), \log\left(\eta_1\right)\right), & \text{continue} \end{cases},$$

where η_0 and η_1 represent the down and upper thresholds, respectively, which are upon the target detection probability P_{D} and false rate P_{F} of the system.

$$\begin{cases} \eta_1 = P_D/P_F \\ \eta_0 = (1-P_F)/P_D \end{cases}.$$

For the detected target, when $\log\left(\Lambda^{\mathrm{FSS}}\left(\mathrm{Z}^k\right)\right)$ falls below the threshold $\log(\eta_0)$, it indicates the target disappearance. The estimation of the target state and its covariance follows:

$$\begin{aligned} \hat{\mathrm{X}}_k &= \sum\nolimits_{l=1}^{N_p} q_k^l \mathrm{X}_{k,l}, \\ \hat{\mathrm{P}}_k &= \sum\nolimits_{l=1}^{N_p} q_k^l \left(\mathrm{X}_{k,l} - \hat{\mathrm{X}}_k\right)\left(\mathrm{X}_{k,l} - \hat{\mathrm{X}}_k\right)^T, \\ q_k^l &= \tilde{q}_k^l \Big/ \sum\nolimits_{l=1}^{N_p} \tilde{q}_k^l, \end{aligned} \tag{15}$$

where $\mathrm{X}_{k,l}$ is the state of the particle l at time k.

Interacting multiple mode PF is successfully applied to track maneuvering weak target. The algorithm as developed by Boers *et al.*[20] incorporates three stages: interaction stage, filtering stage, and combination stage.

Although Boers *et al.*[1,6] have extended the PF algorithm to detect and track two targets through multiple hypotheses testing, it is not suitable for application with more than two variant targets. Let us first consider the situation that the number of the targets is known and fixed as N. The binary hypothesis follows:

H0: no target existent

$$\mathrm{Z}_k^{(i,j)} = \mathrm{n}_k^{(i,j)}.$$

H1: N targets coexistent

$$\mathrm{Z}_k^{(i,j)} = \sum\nolimits_{n=1}^{N} h_k^{(i,j)}\left(\mathrm{X}_k^{(n)}, \mathrm{u}_k\right) + \mathrm{n}_k^{(i,j)}.$$

Assume that the distance from one target to any other is beyond 5Σ, that is to say $\forall \mathrm{X}_k^{(i)}$ and $\mathrm{Y}_k^{(j)}$ $\left(i, j \in \left[1, N\right]\right)$:

$$\left\|x_k^{(i)} - x_k^{(j)}\right\|^2 + \left\|y_k^{(i)} - y_k^{(j)}\right\|^2 \geq \left(5\Sigma\right)^2. \tag{16}$$

Then there is no cell impacted by more than one of the targets simultaneously. And LR of Z_k can be written as

$$\begin{aligned} L\left(\mathrm{Z}_k\left(\mathrm{X}_k^{(1)} \cdots \mathrm{X}_k^{(N)}\right)\right) &= \prod_{i \in C_i\left(\mathrm{X}_k^{(1)}\right)} \prod_{j \in Cj\left(\mathrm{X}_k^{(1)}\right)} \frac{P\left(\mathrm{Z}_k^{(i,j)} \middle| H_1\right)}{P\left(\mathrm{Z}_k^{(i,j)} \middle| H_0\right)} \times \cdots \\ \times \prod_{i \in C_i\left(\mathrm{X}_k^{(N)}\right)} \prod_{j \in C_j\left(\mathrm{X}_k^{(N)}\right)} \frac{P\left(\mathrm{Z}_k^{(i,j)} \middle| H_1\right)}{P\left(\mathrm{Z}_k^{(i,j)} \middle| H_0\right)} &= \prod_{n=1}^{N} L\left(\mathrm{Z}_k\left(\mathrm{X}_k^{(n)}\right)\right). \end{aligned} \tag{17}$$

Let $\mathrm{X}^{(n,k)}$ denote the state of the target n up to time k:

$$\mathrm{X}^{(n,k)} = \left[\mathrm{X}_{k-M}^{(n)}, \cdots, \mathrm{X}_k^{(n)}\right].$$

LR of Z^k with FSS M can be written as

$$\begin{aligned} \Lambda^{\mathrm{FSS}}\left(\mathrm{Z}^k\left(\mathrm{X}^{(1,k)} \cdots \mathrm{X}^{(N,k)}\right)\right) &= \prod_{i=k-M}^{k} \prod_{n=1}^{N} L\left(\mathrm{Z}_i\left(\mathrm{X}_i^{(n)}\right)\right) = \\ \prod_{n=1}^{N} \prod_{i=k-M}^{k} L\left(\mathrm{Z}_i\left(\mathrm{X}_i^{(n)}\right)\right) &= \prod_{n=1}^{N} \Lambda^{\mathrm{FSS}}\left(\mathrm{Z}^k\left(\mathrm{X}^{(i,k)}\right)\right). \end{aligned} \tag{18}$$

Then

$$\log\left(\Lambda^{\mathrm{FSS}}\left(\mathrm{Z}^k\left(\mathrm{X}^{(1,k)} \cdots \mathrm{X}^{(N,k)}\right)\right)\right) = \sum_{i=1}^{N} \log\left(\Lambda^{\mathrm{FSS}}\left(\mathrm{Z}^k\left(\mathrm{X}^{(i,k)}\right)\right)\right). \tag{19}$$

According to Eq. (18), the logarithm of the cumulative LR with N targets coexisting amounts to the sum of the logarithm of the cumulative LR with each one present. Therefore N PF-based detectors each for single target can be built to detect and track N targets one by one on sequential LR testing. However the number of targets is unknown prior, we should build a detecting filtering and a tracking filtering in application. The detecting filter iteratively captures the targets one by one, which starts up after a new target is captured. And the tracking filter maintains and updates the conformed targets. When capturing a new target, the particle of the detector is born on the constraint of the conformed targets state avoiding tracking the same.

In order to attain particles of high quality, the measurements are pre-segmented by a threshold on the target $\mathrm{SNR_P}$. For the detecting filter, new particles are born selectively with positions uniformly distributed around the bins exceeding the threshold and the velocity under the maximum value $v_{\max}$. And the sustaining particles for the tracking filter are updated at each time step. The number of the particles held through the resampling step, after which those particles apart from the central state are deserted:

$$\begin{aligned} \left\{\mathrm{X}_{k,l}^{(n)}\right\} = \Bigg\{ \mathrm{X}_{k,l}^{(n)} \Bigg| &\left(\mathrm{X}_{k,l}^{(n)} - \hat{\mathrm{X}}_k^{(n)}\right)^T \hat{\mathrm{P}}_k^{-1} \times \\ &\left(\mathrm{X}_{k,l}^{(n)} - \hat{\mathrm{X}}_k^{(n)}\right) \leq \gamma, l = 1 \cdots N_p \Bigg\}, \end{aligned} \tag{20}$$

where γ is the gate to ensure that 95% of the particles from the target are kept.

The process noise is vital to the robustness of the algorithm. For the tracking filter, most of the particles converge around the target state. If the covariance of the process noise is too small, the particles predicted are expected to concentrate on the target state. Once the target state waves, the particles hardly cover it resulting in the degeneration of the performance. However, too large covariance leads a mass of barren particles apart from the target state. Given the covariance of the target state estimations P_k and P_{k+1}, the process noise covariance Q_k is adopted as

$$\mathrm{Q}_{k+1} = \begin{cases} \mathrm{Q}_{\min} + \left(\mathrm{Q}_k - \mathrm{Q}_{\min}\right) \times e^{1 - \left(\left\|\mathrm{P}_k\right\| \Big/ \left\|\mathrm{P}_{k-1}\right\|\right)}, \left\|\mathrm{P}_k\right\| \geq \left\|\mathrm{P}_{k-1}\right\| \\ \mathrm{Q}_{\max} + \left(\mathrm{Q}_k - \mathrm{Q}_{\max}\right) \times e^{1 - \left(\left\|\mathrm{P}_{k-1}\right\| \Big/ \left\|\mathrm{P}_k\right\|\right)}, \left\|\mathrm{P}_k\right\| \leq \left\|\mathrm{P}_{k-1}\right\| \end{cases}, \tag{21}$$

where $\mathrm{Q}_{\min}$ and $\mathrm{Q}_{\max}$ are the minimum and maximum of the process noise covariance.

For the detecting filter, the initial particles uniformly distributed convergence around the target through several times of re-sampling. So the target detected time

at that the sequential LR exceeds the upper threshold η_1 lags the target arising time. And the estimated target state at that time differs from the true target state. The difference is fatal for some military application such as missile surveillance. In addition, the detecting filter for new target is started up at the estimated target arising time. The improvement on the estimation provides better performance.

To attain better estimation of the state and time of target arising, an inverted PF based on SLRT with FSS (FSS-SLRT) is implemented through the time target detected to the time t_0 target terminated. And the time of target arising is estimated according to the change degree of the LR, which is given as

$$\hat{t}_{ari} = \left\{k \middle| \arg\max\left(\alpha(k)\right), k \in \left[t_0, t_0 + M\right]\right\}, \tag{22}$$

where $\alpha(k)$is the forward change degree of the LR:

$$\alpha(k) = L\left(\mathrm{Z}^k\right) \Big/ L\left(\mathrm{Z}^{k-1}\right). \tag{23}$$

Similarly the target vanishing time $\hat{t}_{\mathrm{van}}$ is estimated by

$$\hat{t}_{\mathrm{van}} = \left\{k \middle| \arg\max\left(\beta(k)\right), k \in \left[t_1 - M, t_1\right]\right\}, \tag{24}$$

where t_1 is the time when the FSS-SLRT is terminated and $\beta(k)$is the backward change degree of the LR:

$$\beta(k) = L\left(\mathrm{Z}^{k-1}\right) \Big/ L\left(\mathrm{Z}^{k}\right). \tag{25}$$

The algorithm was tested on the simulated data of a scenario with three targets, which consists of 40 frames: target-1 at $\mathrm{SNR_P}$ -2.2 dB arisen at frame 5 with the initial state [15.5, 1.1, 15.5, 0.2, and 7.8] T, which moved for 10 s with a CV model and then switched to C-CT model for another 10 s. And it switched to CV again for 10 s and vanished at frame 35. Target-2 at $\mathrm{SNR_P}$ 2.3 dB arisen at frame 5 with the initial state [25.4, –1.1, 20.8, 0.1, and 9.8] T, which moved for 10 s with a CV model and then switched to AC-CT model for the next 10 s. And it switched to CV again for 10 s and disappeared at frame 35. Target-3 at $\mathrm{SNR_P}$ –2.2 dB moved from frame 10 to frame 30 with the initial state [20, 0.1, 35.5, –1.2, and 7.8] T and the CV model.

The size of the image was 60×60 and the target spread was $\Sigma = 0.7$. The frame time step was $T = 1$ s. The detection performance indicator were defined as $P_{\mathrm{D}} = 0.9$ and $P_{\mathrm{F}} = 1 \times 10^{-5}$. Targets maneuvering angular rate was $\omega = 0.314$ rad/s. The process noise covariance Q was defined as in Ref. [21] with $q_{\mathrm{s}} = 0.001$ and $q_{\mathrm{i}} = 0.01$. The minimum and the maximum of the additive process noise were set to 0.5 and 10 Q. The amplitude noise variance σ^2 was set to 1 and the detection probability P_{D} was set to 0.995. The number of particles for tracking filter was chosen to be 4000. And the number of the particles for detecting filter was chosen to be 8000 with the half representing the new born particles at each frame and the rest half representing the sustaining particles. After the re-sampling, only 4000 particles were held. The variance of the focal plane array imaging errors was 0.05 bin both in x and y dimensions. The FSS for the SLRT was 6 and the upper and down thresholds were set to $\eta_1 = 9 \times 10^4$ and $\eta_0 = 10$. And the maximum velocity $v_{\max}$ for the particles to be initialized is set to be 5 pixels/frame. Hundred Monte Carlo trials were conducted. The mode transition matrix was given by

$$\Pi = \begin{bmatrix} 0.8 & 0.1 & 0.1 \\ 0.3 & 0.6 & 0.1 \\ 0.3 & 0.1 & 0.6 \end{bmatrix}.$$

In order to reduce the complexity, the raw image data are pre-segmented by a very low threshold to get the cells, in which the target might locate. And the particles sampled for new born targets are uniformly distributed around the cells.

The map of the data set at frame 10 is shown in Fig. 1(a) with target-1 centered at pixel (20, 16), target-2 centered at pixel (20, 21), and target-3 centered at pixel (20, 35). The true traces and the detected traces are shown in Fig. 1(b). It can be seen that the total three targets are detected and tracked successfully.

The mode probability estimated of the three targets at each time step is shown in Fig. 2. It validates the algorithm efficiency to estimate the target motion model. Among the 100 Monte Carlo trials, three targets were fully detected with no false traces.

The root mean square (RMS) errors in position and amplitude are calculated according to

$$\text{RMS error}_k = \sqrt{\frac{1}{N_c}\sum_{i=1}^{N_c}\left[\left(x_k - \hat{x}_{k,i}\right)^2 + \left(y_k - \hat{y}_{k,i}\right)^2\right]}, \tag{26}$$

$$\text{amplitude error}_k = \sqrt{\frac{1}{N_c}\sum_{i=1}^{N_c}\left(I_k - \hat{I}_{k,i}\right)^2}, \tag{27}$$

where x_k and y_k are the true target positions at time k, $\hat{x}_{k,i}$ and $\hat{y}_{k,i}$ are the estimated target positions of iteration i, I_k is the target amplitude along with its estimation $\hat{I}_{k,i}$, and N_c is the number of the Monte Carlo trials.

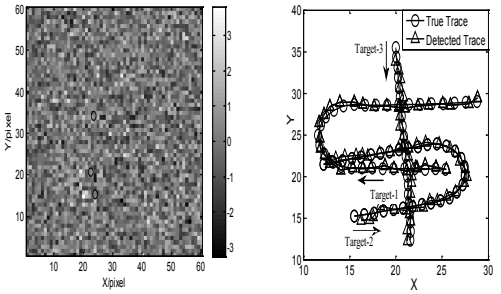

(a) (b)

Fig. 1 (a) Map of the data set for three targets ('O') and (b) multi-target traces.

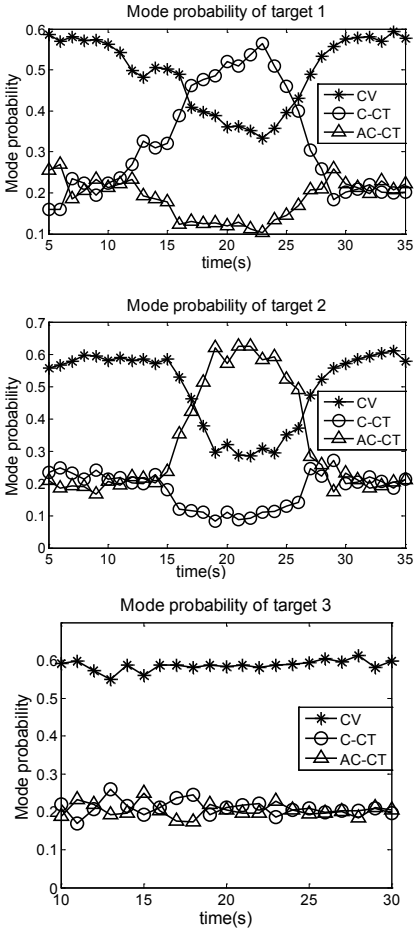

Fig. 2. Mode probability estimations of three targets.

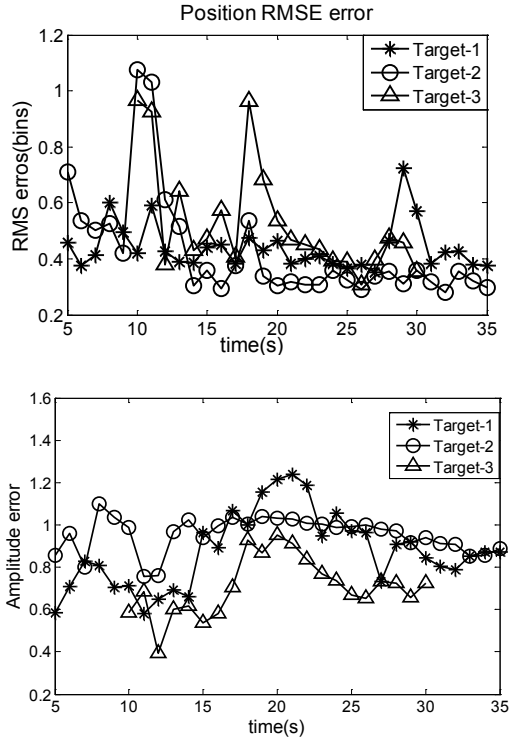

Fig. 3. RMS error in position and amplitude.

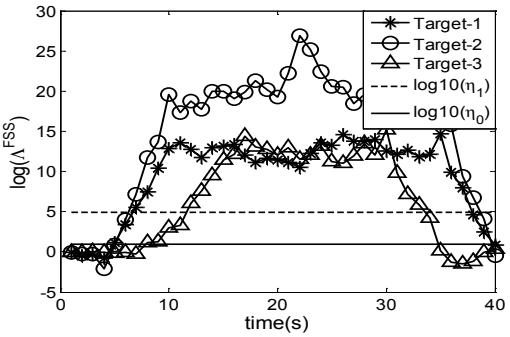

Fig. 4. Logarithmic of $\Lambda^{\text{FSS.}}$

The performances of the algorithm in terms of the RMS in position and in amplitude are shown in Fig. 3. It can be seen that the error of the targets position estimation at the time targets arisen was depressed through the inverted PF. But the peaks took on as the time targets were detected.

The FSS-SLRT is shown in Fig. 4. It displays that not only the time targets are detected but also the time targets are terminated, respectively, lagged the true time targets arisen and vanished.

The forward and backward change degrees of the LR for three targets are shown in Fig. 5. The peaks of α took on at the time targets arisen and the peaks of β took on at the time targets vanished.

The averaging estimation of the time targets arisen and vanished is listed in Table 1. It can be seen that the estimation on the change degree of the LR is much better than that on FSS-SLRT.

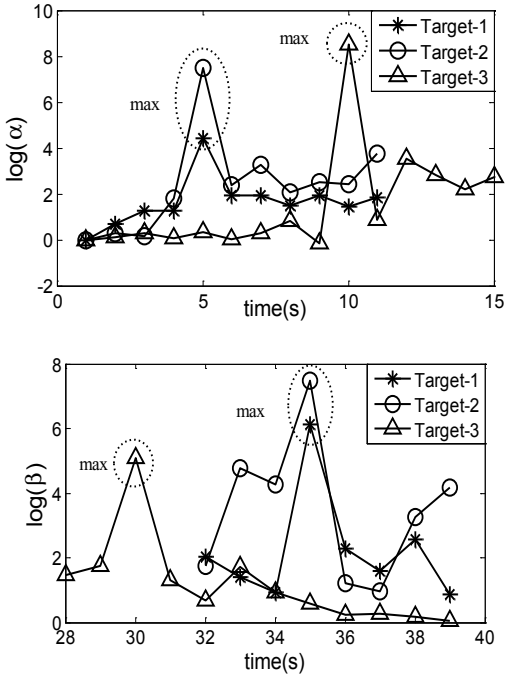

Fig. 5. Logarithmic of α and β for three targets.

Table 1. Comparison of the Estimation of the Time Targets Arisen and Vanished

	Targets arisen (s)			**Targets vanished (s)**		
Target	1	2	3	1	2	3
True	5	5	10	35	35	30
FSS-SLRT	9.1	7.8	14.2	38	38	34
Presented	6.8	5.4	11	35.1	34.8	29.9

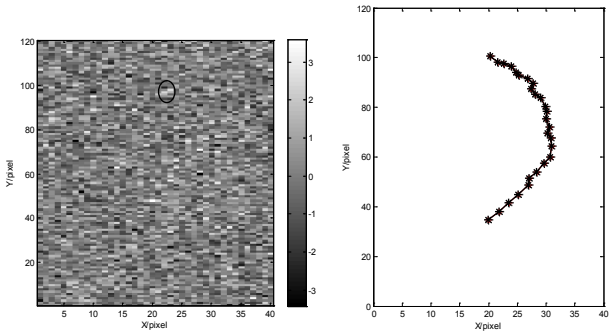

Fig. 6. Map of the data set for one target ('○') and target trace.

Further we compare the presented algorithm with the PF, which is combined with multi-model. The algorithms are tested on the simulated data of a scenario with one target at SNR_P 3.8 dB. The raw data and target trace are depicted in Fig. 6.

The detected target trace and the RMS error are depicted in Fig. 7. It seems that the presented algorithm can accurately track the target trace with better performance over MM-PF in RMS error especially at the time the target arise and vanish.

In conclusion, we introduce a PF-based TBD algorithm for multiple targets with optimization through selectively particles sampling and additive process noise. The algorithm improves the estimation of the target arising and vanishing time and state, which gives satisfactory performance on the simulated data with three maneuvering targets at different SNRs. Although it is assumed that multiple targets do not encounter in a cell, it is able to track multiple targets with collision for the constraint on the new born particles.

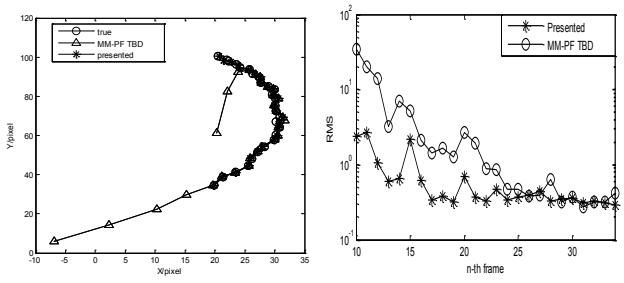

Fig. 7. Detected target trace and RMS error in position.

References

1. Y. Boers and H. Driessen, IEEE Signal Process. Lett. **10,** 300 (2003).
2. S. J. Davey and M. G. Rutten, in *Proceedings of IEEE* 342 (2007).
3. R. L. Streit, M. L. Graham, and M. J. Walsh, Digital Signal Process. **12,** 394 (2002).
4. A. Pakfiliz and M. Efe, in *Proceedings of IEEE Conference and Systems Engineering* 1 (2005).
5. T. Kirubarajan and Y. Barshalom, in *Proceedings of IEEE* 536 (2004).
6. Y. Boers and J. N. Driessen, IEE Proc. Radar Sonar Navig. **151,** 351 (2004).
7. P. Pertilä, in *Proceedings of IEEE International Conference on Acoustics, Speech and Signal Processing ICASSP* 4974 (2010).
8. M. Morelande, C. Kreuchetr, and K. Kastella, IEEE Trans. Signal Process. **55,** 1589 (2007).
9. S. Buzzi, M. Lops, and L. Venturino, IEEE Trans. Aerosp. Electron. Sys. **44,** 1150 (2008).
10. D. Orlando, L. Venturino, and L. Marco, IEEE Tans. Signal Process. **58,** 933 (2010).
11. D. Orlando, F. Ehlers, and G. Ricci, *in Proceedings of 2nd International Workshop on Cognitive Information Processing* 180 (2010).
12. D. Orlando, G. Ricci, and Y. Bar-Shalom, IEEE Trans. Aerosp. Electron. Syst. **47,** 1837 (2011).
13. R. Mahler, IEEE Trans. Aerosp. Electron. Syst. **39,** 1152 (2003).
14. B. N. Vo, S. Singh, and A. Doucet, IEEE Trans. Aerosp. Electron. Syst. **41,** 1224 (2005).
15. K. Punithakumar, T. Kirubarajan, and A. Sinha, IEEE Trans. Aerosp. Electron. Syst. **44,** 87 (2008).
16. K. Punithakumar, T. Kirubarajan, and A. Sinha, Proc. SPIE **5913,** 59131s (2005).
17. Y. L. Long, H. Xu, W. An, et al. Chin. J. Aeronaut. **25,** 252 (2012).
18. Z. P. Lin, Y. Y. Zhou, and W. An, J. Infrared Millim. Waves **5,** 475 (2012).
19. X. R. Li and V. P. Jinkov, IEEE Trans. Aerosp. Electron. Syst. **39,** 1333 (2003).
20. Y. Boers and J. N. Driessen, IEE Proc. Radar Sonar Navig. **150,** 344 (2003).
21. M. Rutten, B. Ristic, and N. Gordon, in *Proceedings of International Conference on Information Fusion* 169 (2005).
22. D. J. Salmond and H. Birch, in *Proceedings of the American Control Conference* 3755 (2001).